Determining the Conformation of an Adsorbed Br-PEG-Peptide by Long Period X-ray Standing Wave Fluorescence

Carrie A. Crot[a], **Chunping Wu**[a], **Mark L. Schlossman**[b,a*], **Thomas P. Trainor**[c], **Peter J. Eng**[d], and **Luke Hanley**[a*]

a*Department of Chemistry, University of Illinois at Chicago, Chicago, IL 60607-7061*

b*Department of Physics, University of Illinois at Chicago, Chicago, IL 60607*

c*Department of Chemistry and Biochemistry, University of Alaska Fairbanks, Fairbanks, AK 99775*

d*Center for Advanced Radiation Sources, The University of Chicago, Chicago, IL 60603*

Abstract

Long period x-ray standing wave fluorescence (XSW) and x-ray reflectivity techniques are employed to probe the conformation of a Br-polyethylene glycol (PEG)-peptide adsorbate at the hydrated interface of a polystyrene substrate. The Br atom on this Br-PEG-peptide construct serves as a marker atom allowing determination by XSW of its position and distribution with respect to the adsorption surface with angstrom resolution. Adsorption occurs on native or ion beam modified polystyrene films that are spin coated onto a Si substrate and display either nonpolar or polar surfaces, respectively. A compact, oriented monolayer of Br-PEG-peptide can be formed with the peptide end adsorbed onto the polar surface and the PEG end terminating with the Br tag extending into the aqueous phase. The 108 – 141 Å distance of the Br atom from the polystyrene surface in this oriented monolayer is similar to the estimated ~150 Å length of the extended Br-PEG-peptide. This Br-polystyrene distance depends upon adsorption time and surface properties prior to adsorption. Incomplete multilayers form on the polar surface after sufficient adsorption time elapses. By contrast, adsorption onto the nonpolar surface is submonolayer, patchy, and highly disordered with an isotropic Br distribution. Overall, this combination of x-ray surface scattering techniques with a novel sample preparation strategy has several advantages as a real space probe of adsorbed or covalently bound biomolecules at the liquid-solid interface.

I. Introduction

The adsorption of proteins, peptides, and other molecular species onto the surfaces of biomaterials is of fundamental importance in tissue engineering, biosensors, immunoassays and protein arrays.[1–3] Protein adsorption occurs immediately once a biomaterial is brought into contact with physiological fluid and thus transpires well before cells arrive at the surface. Cells therefore interact with this interfacial protein layer rather than with the native biomaterial surface. The importance of these adsorption events has lead many studies to focus on the correlation between surface properties, protein adsorption, and cellular response.[4–7]

Protein adsorption onto solid surfaces has been examined by various surface science techniques including quartz crystal microbalance, x-ray photoelectron spectroscopy (XPS), Fourier transform infrared spectroscopy, atomic force microscopy, time of flight secondary ion mass spectrometry, and matrix assisted laser desorption ionization mass spectrometry.[1–3] These

*Corresponding author email: lhanley@uic.edu.

techniques provide useful surface chemical information, sometimes even with high spatial resolution. However, it is often difficult to extract unambiguous structural information on adsorbed proteins and other species from such techniques. An additional shortcoming of vacuum based surface analysis techniques is that dehydration can lead to denaturing of the adsorbed layer, thereby perturbing the interfacial composition and structure. Consequently, it is essential to perform *in situ* studies of molecular adsorption to complement the information provided by vacuum based methods.

Synchrotron based x-ray methods are powerful real-space structural probes of adsorption processes at the solid-aqueous solution interface because of the intensity, collimation, polarization, and immense penetrative power of synchrotron radiation.[8–11] The tunable nature of synchrotron radiation also permits the use of element specific spectroscopic methods, allowing one to investigate various marker atoms in an adsorbed species. Long period x-ray standing wave fluorescence (XSW) and x-ray reflectivity techniques are employed in this work to probe the conformation of molecular adsorbates at the hydrated interface of synthetic biomaterials. Specular x-ray reflectivity can resolve several surface parameters including interfacial roughness, film thickness, and electron density at the angstrom scale.[12–16] The surface roughness of buried interfaces can be investigated by x-ray reflectivity without cross-sectioning, a unique capability amongst surface analytical techniques. However, x-ray reflectivity is not sensitive to trace distributions of elements within a film, indicating the importance of an additional element specific technique such as XSW. XSW is based on the principle that the fluorescence yield of a marker atom within a film is proportional to the strength of the electric field which varies as a function of the incident x-ray angle.[17–20] Monitoring the intensity of the fluorescence yield allows the determination of the location and distribution of the marker atom with respect to the surface plane. XSW techniques have the advantage of element specificity and can provide information on the distribution of trace species under aqueous solution with angstrom resolution. XSW has been successfully applied to the characterization of various interfacial problems including membrane protein adsorption, Langmuir-Blodgett films, self-assembled monolayers, biofilms on mineral surfaces, and polymer films.[8,10,19–23]

The present study applies XSW to probe the conformation of a model peptide construct at the solid-liquid interface. A bromine (Br) labeled-peptide-polyethylene glycol construct is used to mimic the adsorption of small biological molecules. A 15 residue peptide is employed that contains the Arg-Gly-Asp (RGD) motif shown to enhance cell attachment and growth.[24–26] Finally, the polyethylene glycol (PEG) end of the construct is covalently bound with a Br labeled phenylalanine (Phe or F) amino acid, which is used as the marker atom and fluorescent tag. The Br-PEG-peptide construct is designed such that the end of the peptide is expected to adsorb onto a polar surface with the PEG extending into the aqueous phase terminated by the Br atom (away from the surface). The XSW experiments are designed to test this hypothesized conformation of the Br-PEG-peptide construct. The Br-PEG-peptide is adsorbed onto a flat, polar, amine-functionalized polystyrene film that is spin coated onto a flat silicon (Si) substrate. Measurements of the Br fluorescence yield as a function of incident angle provides information on the distance of the Br layer from the Si surface with ~10 Å resolution in the current experimental configuration.

A polystyrene spacer is used to increase the distance of the Br-PEG-peptide from the Si substrate. The critical period or XSW period at the critical angle for total external reflection of Si is ~200 Å. Therefore the ~250 Å thick polystyrene spacer layer allows multiple standing wave antinodes to pass through the Br tagged peptide layer,[16] thereby increasing the information available from the fluorescence yield profile.

The polystyrene surface is amine-functionalized via the deposition of hyperthermal, non-mass selected allylamine ions. The polyatomic ion deposition technique has been discussed extensively in prior work.[16,27–29] Polyatomic ion deposition is analogous to the radiative oxidation of native polystyrene used to produce the common cell growth substrate known as tissue culture polystyrene.[30] It is found that polyatomic ion deposition produces an oxidized, amine-functionalized polystyrene surface which is polar and flat on an angstrom scale over the ~1 cm length of the x-ray footprint.

II. Experimental Details

A. Preparation of Br-PEG-Peptide Adsorbed to Polar and Nonpolar Surfaces

The preparation of similar films by polyatomic ion deposition has been explained previously and will only be summarized here.[28,29] Si(100) wafers that are 6 mm thick and have a diameter of 25 or 50 mm (Semiconductor Processing, Boston, MA) are cleaned and oxidized to produce a uniform ~15 Å thick oxide layer.[31] Polystyrene thin films are then prepared on the Si wafers by spin coating a 0.6% solution of polystyrene (molecular weight: 2,330 Da, Aldrich, Milwaukee, WI) in CH_2Cl_2 for 1 min at 6000 rpm.[16,31] The thickness of the polystyrene layer was previously determined by x-ray reflectivity to be ~250 Å.[16] The surface cleanliness and uniformity of the polystyrene film are examined via survey and valence band x-ray photoelectron spectra, as described previously.[32]

Amine-functionalized polystyrene is produced via non-mass selected deposition of allylamine ions under vacuum using a broad beam Kaufman ion source.[28] Allylamine is the precursor gas used to produce gaseous ions with kinetic energies of either 50 or 200 eV. Fragmentation of allylamine ions in the source is monitored by an energy analyzer/quadrupole mass spectrometer, which finds that fragmentation of the parent ion increases with ion energy. Similar fragments are obtained for both ion energies, but their relative abundances vary significantly. A larger abundance of the parent ion at m/z 56 and 57 corresponding to $[CH_2=CH-CH_2-NH_{1-2}]^+$ and a m/z 39 fragment corresponding to $[C_2NH]^+$ are formed at 50 eV. A higher abundance of low mass fragments are formed at 200 eV, including m/z 39, m/z 30 corresponding to $[CNH_4]^+$ and m/z 28 corresponding to $[CH_2N]^+$ or $[C_2H_4]^+$. 50 eV allylamine ions are produced using the following parameters in the broad beam ion source: ~7 A cathode current, ~40 eV discharge voltage, 50 µA beam current, ~1 µA ion current on the substrate, and 10 min deposition time. Similar parameters are used to produce 200 eV allylamine ions except that the beam current is 2.5 mA and the ion current on the substrate is ~30 µA.

The Br-PEG-peptide construct used in this study is composed of the amino acid sequence Ac-F(PEG)$_{33}$GEEGYGRGDSPG-Am, and is synthesized in house (Protein Laboratory, Research Resource Center, University of Illinois at Chicago) from phenylalanine (F) amino acid that contains a Br atom (Fmoc-L-4-bromophe, Peptech Corp., Burlington, MA) and PEG (O-(N-Fmoc-2-aminoethyl)-O'-(2-carboxyethyl)-undecaethylene glycol, Nova Biochem, Darmstadt, Germany).

The peptide is dissolved in 0.1 M sodium phosphate buffer to a concentration of 100 µM. The amine-functionalized surfaces are equilibrated with the buffer solution prior to adding the Br-PEG-peptide solution to the surface. The time allowed for peptide adsorption is varied from 0.5 to 10 hr, after which the polystyrene surface is rinsed with buffer solution and de-ionized water, then dried in a He gas flow. Br-PEG-peptide samples so prepared are immediately analyzed as described below.

B. X-ray Photoelectron Spectroscopy (XPS)

Details of the x-ray photoelectron spectrometer and data analysis used for analysis of the substrates prior to adsorption are only summarized here since a full description has been previously published.[32] A monochromatic Al-Kα x-ray source (model VSW MX 10 with 700 mm Rowland circle monochromator, VSW Ltd., Macclesfield, Cheshire, UK) is utilized to perform XPS experiments (15 keV, 25 mA emission current) with a 150 mm concentric hemispherical electron energy analyzer (model Class 150, VSW) equipped with a multichannel detector operated at constant energy mode. The photoemission is measured normal to the surface and the pass energy is 22 eV corresponding to ~0.75 eV energy resolution. All binding energies are referenced to the C(1s) (aliphatic/aromatic) core level peak of native polystyrene at 285.0 eV which is used as a charge reference for all other photoemission peaks. Peak fitting is performed with Spectra software (VSW), using Shirley background and a 35:65 ratio Lorentzian:Gaussian product line shape, with corrections for analyzer transmission function. Three samples are analyzed and averaged for each ion energy. Error bars on the data correspond to the standard deviation for the analysis of different data sets.

XPS analysis of Br-PEG-peptide adsorption onto 50 eV ion modified polystyrene coated Si wafer is acquired utilizing a commercial instrument (Kratos Axis 165, Manchester, UK) equipped with a monochromatic Al-K$_α$ source (15keV, 10mA emission current), a 165 mm radius hemispherical analyzer, and an eight channeltron detection system operated at constant energy mode. The photoemission angle is measured normal to the surface and the pass energy is 160 eV for the survey scans and 40 eV for the core level scans. Charge neutralization is performed using the following conditions: 1.7 A filament current, 2.6 eV charge balance, 1.3 eV filament bias. Peak fitting is performed with Vision software (Kratos), using a Shirley Background and a 30:70 ratio Lorentzian:Gaussian product line shape, with a correction for analyzer transmission function.

C. Atomic Force Microscopy (AFM)

Surface morphologies of the amine-functionalized polystyrene surfaces are measured by AFM (model Nanoscope IIIA, Digital Instruments, Santa Barbara, CA), utilizing tapping mode and phase contrast for highest spatial resolution.[16,28] Tapping mode is applied to avoid destruction of the sample. Four 1×1 µm areas are scanned for each ion energy. The instrument software calculates the RMS roughness for each spot and then the average is taken for each sample.

D. X-ray Standing Wave Fluorescence and X-ray Reflectivity

Long period x-ray standing wave fluorescence spectroscopy (XSW) and x-ray reflectivity measurements are conducted on undulator beamline 13-ID-C located at the GeoSoilEnviroCARS sector of the Advanced Photon Source (APS), Argonne National Laboratory (Argonne, IL). An incident energy of 14.8 keV is produced using a liquid nitrogen cooled double crystal Si (111) monochromator with Rh-coated double focusing mirrors.[33,34] The x-ray beam is collimated to 1.8 mm vertical and 20 µm horizontal.

Samples are placed in a vapor controlled Teflon sample cell which is covered with polypropylene film. The sample cell is purged with helium passed through water bubblers to create a humid environment (relative humidity >95%) during experiments, thereby hydrating the adsorbed Br-PEG-peptide. The incident (I_0) and reflected (I_1) x-ray intensity are monitored by using nitrogen-filled gas ionization chambers. Fluorescence spectra are acquired using a 13-element Ge solid state array detector (Canberra Industries, Meriden, CT) coupled to a digital x-ray processor electronics (X-Ray Instrumentation Assoc., Newark, CA) as the incidence angle is scanned from 0 to 0.35 degrees, which corresponds to range of $0 - 0.916$ Å^{-1} in q_z space, using step sizes of $0.001° - 0.005°$. The step size is determined to allow collection of all significant fluorescence features. The deadtime corrected fluorescence yield spectrum from

each detector element is averaged and the total area of Br K_α peak at 11.9 keV is integrated using a Gaussian peak line shape on a linear background. The background subtracted data is normalized to the incident intensity (I_o), with a footprint correction applied.[10] A relative scale factor is applied to further normalize the data to unit intensity at $\theta \approx 0.2°$

Total external reflection conditions are employed to produce a standing wave above the surface that has a defined period,

$$D = \lambda/(2\sin\theta_i) \tag{1}$$

where θ_i is the incident angle and 2θ is the angle between the incident and reflected beam wave vectors. The standing wave is generated due to the coherent interference of the incident and reflected beam. The intensity of the standing wave will oscillate as a function of incident angle, which for a standing wave generated in vacuum above a mirror surface can be described as

$$I_{sw}(q_z,z) = |E_o|^2 \left[1 + R + 2\sqrt{R}\cos(\nu - q_z z) \right] \tag{2}$$

where $R = |E_R/E_o|^2$, $\nu = \arg(E_R/E_O)$, and $q_z = 4\pi\sin\theta_i/\lambda$. $I_{SW}(q_z,z)$ is the intensity of the standing wave, E_O and E_R are the complex electric field amplitudes of the incident and reflected beam at the mirror/vacuum interface, q_z is the magnitude of the wave vector transfer along the z axis, and ν is the phase shift between the incident and reflected beam. $I_{SW}(q_z,z)$ is calculated based on the optical properties of the sample using a matrix method.[35] The Br atoms will fluoresce if the x-ray energy exceeds the binding energy of the inner shell electrons, due to the photoelectric effect. The fluorescence yield, $Y(q_z,z)$ profile can be described by

$$Y(q_z,z) = \int I_{sw}(q_z,z) N(z) dz \tag{3}$$

where a Gaussian function is used for N(z) to describe the distribution profile of the Br atoms averaged over the x-y plane.

X-ray reflectivity is collected simultaneously with the x-ray fluorescence data, using a bicron detector. The reflectivity data measured consists of the x-ray intensity reflected from the sample normalized to the incident intensity measured just prior to the x-rays striking the sample surface. X-ray reflectivity curves are used to estimate the thickness, roughness, and relative density of the polystyrene and Br-PEG peptide films, which are fixed as input parameters in the subsequent fitting of the XSW data. X-ray reflectivity measurements are performed prior to and following each XSW measurement to monitor the possible organic film degradation by radiation damage, as discussed further below. Multiple data sets are collected for each sample with each new data set acquired at a fresh spot on the sample, unless otherwise noted. The reported fitting parameters are the average of at least three separate data sets, except for the two data sets each used to obtain averages for the nonpolar and dry surfaces.

III. Results & Discussion

A. Preparation and Characterization of Nonpolar and Polar Surfaces for Adsorption

Figure 1 depicts the process used to produce both nonpolar (native polystyrene) and polar (amine-functionalized polystyrene) surfaces subsequently used for adsorption of Br-PEG-peptide. First, Si wafers are cleaned and oxidized[31] to produce a uniform oxide layer that is ~15 Å thick with 2 Å RMS surface roughness measured by AFM. A polystyrene layer is then spin coated onto the Si wafer under conditions previously shown by x-ray reflectivity and AFM to produce a film of thickness of ~250 Å and roughness of 2 Å RMS.[16]

Next, the surface of the polystyrene film is functionalized with a mixture of primary and secondary amine groups by non-mass selected ion deposition of gaseous allylamine ions at either 50 or 200 eV kinetic energy. Table 1 summarizes the elemental percentages that are

obtained via XPS for the clean oxidized Si wafer, spin coated polystyrene layer, and amine-functionalized polystyrene. The nitrogen and carbon content in the amine-functionalized polystyrene are consistent with the formation of amine and other nitrogen containing groups on the surface, at higher concentrations from 50 eV ion deposition compared with 200 eV ion deposition. Previous work with mass-selected allylamine ions found that primary amine content was higher for deposition at lower ion energies.[29] Water and air exposure of the amine-functionalized films also is expected to form hydroxyl and other oxygenated species on the two amine-functionalized surfaces, albeit to a different extent.

Table 1 also illustrates that the surface roughness increases directly with the kinetic energy of the allylamine ions, from 3 to 6 Å RMS, due to an increase in fragmentation of both the allylamine ions and the polystyrene layer with ion energy.[16] X-ray reflectivity verifies that allylamine ion deposition onto polystyrene produces a surface with roughnesses on the angstrom scale over the macroscopic length scale of the x-ray footprint (data not shown).

B. Verification of Method: Fitting, Adsorbate Hydration, and Radiation Damage

Several steps in the XSW experiment must be verified before the results on adsorbate conformation can be evaluated. The data fitting procedure, the method employed to hydrate the adsorbate during x-ray surface scattering, and x-ray radiation damage to the sample are discussed in this section.

The general strategy for fitting the x-ray data is to use x-ray reflectivity to obtain the film thickness, roughness, and relative density parameters which are then used as input for the fitting of the fluorescence yield profiles. Off-specular reflectivity was not measured due to the time constraint of limiting radiation damage (see below) and so background scattering is not used to correct the reflectivity scans. Thus, the primary use of the reflectivity is to determine the thickness of each layer. The roughness values are also obtained by fitting the reflectivity data and are lower limits of the actual interfacial roughnesses.

The samples are modeled as a three-layer composite consisting of the Br-PEG-peptide layer of variable thickness, a polystyrene layer, and the Si substrate, as indicated in Figure 1. A $0.121°$ critical angle of Si for total reflection is used to fit all of the data sets and the reflectivity scale is normalized to unity below the critical angle. The allylamine layer is modeled as part of the polystyrene layer since the two cannot be readily distinguished by x-ray reflectivity due to their lack of electron density contrast. Each layer is defined by the parameters of thickness, interfacial roughness, relative density, and refractive index. The absorption code of Brennan and Cowan[36] is used to calculate the refractive index for a fixed, reference bulk density of each layer. A Debye-Waller model is used to account for the interfacial roughness. The refractive indices and interfacial roughnesses are held constant during the fit while the film thicknesses and relative densities are varied. The complex refractive index is $2.209 \times 10^{-6} + 1.541 \times 10^{-8}(i)$ for the Si layer; $1.173 \times 10^{-6} + 3.975 \times 10^{-10}(i)$ for the combined polystyrene and allylamine layer and $1.153 \times 10^{-6} + 6.942 \times 10^{-10}(i)$ for the Br-PEG-peptide layer. Each layer is characterized by its refractive index multiplied by its relative density ratio to scale the layer.

Figure 2 (a) displays the x-ray reflectivity data collected for Br-PEG-peptide adsorbed for 2.5 hr on the smooth polar surface, formed by 50 eV allylamine ion deposition onto polystyrene. The two spectra displayed in Figure 2 only vary in that the relative humidity of the He gas blown across the substrate is either 0% or ~95%. Hydration of the Br-PEG-peptide layer is apparent from the increases in thickness for the humidified film which is evident from the change in the period in the large oscillations. Fits to the data in Figure 2 are shown in Table 2 and are made assuming the thickness of the bulk, hydrophobic polystyrene layer remains constant for the dry and hydrated films at 250 Å. The fitting indicates that the Br-PEG-peptide

film thickness on this smooth polar surface increases from 140 to 156 Å with hydration, suggesting that water is incorporated into the hydrated peptide layer. Figure 2 (b) illustrates the Br fluorescence yield profiles of the relatively dry versus hydrated Br-PEG-peptide again adsorbed for 2.5 hr onto the smooth polar surface. Hydration of the Br-PEG-peptide sample is obvious in the fluorescence yield profiles due to a shift in the peaks by 0.0012° to lower incident angle. Fitting of the fluorescence yield profiles indicates the Br-polystyrene surface distance increases from 129 to 141 Å under humid He, again indicating that water is incorporated into the peptide layer. This hydration strategy avoids x-ray scattering through a macroscopic water layer, which considerably complicates data analysis. All x-ray scattering results discussed below are recorded under humid He vapor.

The fits in Figure 2 (a) match the phase and amplitude of the reflectivity data, except at higher scattering angles. The slight miss-fit at larger scattering angle could be a result of thickness variations in the film or background scattering, which in turn will lead to an underestimate of the interfacial roughness values. The poorer match between fit and data at higher scattering angles may also arise from variations in Br-PEG-peptide layer thicknesses that may also occur here. Nevertheless, the parameters derived from these fits provide a good model for analysis of the XSW data, thus indicating a relatively minor impact of the high scattering angle miss-fit.

X-ray reflectivity is also used to assess radiation damage of the samples. Figure 3 displays x-ray reflectivity scans of Br-PEG-peptide adsorbed for 2.5 hr to the smooth polar surface, collected successively at the same position on a single sample. Each individual reflectivity scan is acquired within ~7 min and there is ~35 min of x-ray beam exposure between the first and last scan displayed in Figure 3. Analysis of the x-ray reflectivity data indicates that the Br-PEG-peptide film thickness decreases from 168 to 159 Å by the commencement of the fifth scan. This indicates that ~30 min of x-ray exposure is allowable here before damaging the sample, sufficient time to collect two reflectivity scans separated by measurement of the fluorescence yield profile. Comparison of these two reflectivity scans for a given sample spot is used to verify that the sample is not significantly altered by radiation damage within the analysis time. Subsequent experiments showed further attenuation of the x-ray beam permits measurements with dramatically lower beam damage (data not shown). Thus, it is found that radiation damage can be controlled despite the susceptibility of this adsorbate system to such unintentional modification. Translating the sample to analyze a fresh spot on the film is also used here, as it was shown previously to minimize radiation damage of Langmuir-Blodgett films.[37]

C. Conformation of Adsorbed Br-PEG-Peptide

The peptide construct was designed such that the peptide end should adsorb onto a polar surface with the PEG end extending into the aqueous phase with Br at the farthest point from the substrate. Given the expected ~150 Å length of an extended Br-PEG-peptide, the Br distance from the Si substrate under this adsorbate configuration would be approximately twice the critical period of Si, allowing two antinodes to traverse through the Br layer as the incident angle is increased up to the critical angle. X-ray scattering confirms this hypothesized conformation at the solid-aqueous interface of the polar surface under conditions described further below. The native polystyrene film is referred to below as the nonpolar surface. 50 and 200 eV allylamine ion deposition onto polystyrene are referred to below as the smooth and rough polar surfaces, respectively.

Figure 4 (a) displays x-ray reflectivity scans for Br-PEG-peptide on the smooth polar surface for adsorption times of 0.5, 2.5, and 10 hr. Drastic differences in the reflectivity scans are apparent as the Br-PEG-peptide adsorption time is increased. The 0.5 hr adsorption displays a polystyrene film thickness of 248 Å and a Br-PEG-peptide thickness of 116 Å. The thickness

of the polystyrene is held constant at 250 Å during the fitting process, whereupon the Br-PEG-peptide layer thickness is found to increase to 156 Å for a peptide adsorption time of 2.5 hr. This increase in the peptide layer thickness with adsorption time strongly suggests the growth of a full monolayer after several hours.

Analysis of the fluorescence yield profiles indicates growth of a compact monolayer within 2.5 hr adsorption, in agreement with the reflectivity data. The XSW data also indicates that the Br-PEG-peptide adsorbs with the peptide end down on the polar surface with Br extending into the aqueous phase. Figure 4 (b) illustrates the Br fluorescence yield profiles as a function of Br-PEG-peptide adsorption time on the smooth polar surface, which are fit to generate the Br spatial distribution with respect to the Si surface. The maxima in the fluorescence yield profiles are shifted by 0.0015° to a lower incident angle as the adsorption time increases, indicating an increase in the distance of the Br-polystyrene surface distance. The reduction in fluorescence signal beyond the critical angle of Si is due to the abrupt decrease in the reflected beam intensity in this region. There are slight differences between the two shorter adsorption times. The Br-polystyrene surface distance increases from 108 Å for 0.5 hr adsorption to 141 Å for 2.5 hr adsorption, while the distribution width decreases slightly from 13 to 10 Å.

These Br-polystyrene surface distances are consistent with formation of a compact monolayer with the peptide end adsorbing to the polar surface and Br extending away from the surface, especially given that the length of the fully extended Br-PEG-peptide is ~150 Å. XPS data on the adsorbed Br-PEG-peptide also supports the formation of a monolayer: 0.5 hr of adsorption onto the smooth polar surface displays 0.10 ± 0.02 % Br, 2.5 hr of adsorption displays 0.17 ± 0.01%, and 10 hr of adsorption displays 0.18 ± 0.01 % Br. While the precise adsorption time at which monolayer formation is complete has not been determined here, the leveling off of surface Br content at 2.5 hr is consistent with monolayer formation. No Br is observed on the smooth polar surface prior to adsorption of the Br-PEG-peptide.

Figure 4 (a) also displays x-ray reflectivity for the 10 hr adsorption which appears distinctly different from the corresponding data for the shorter adsorption time. The thickness of the peptide layer increases to 449 Å for the 10 hr adsorption, indicating the presence of a thicker and/or an additional layer. The primary oscillations in the 10 hr reflectivity data also begin to dampen out, suggesting formation of an incomplete multilayer atop the monolayer. The 449 Å Br-PEG-peptide layer thickness corresponds to three layers, but the 12 Å roughness of this multilayer may be underestimated, leading to an over estimate of the film thickness and an under estimate of the relative density.

A dramatic change in the XSW is also observed between 2.5 and 10 hr with the Br-polystyrene surface distance increasing to 332 Å with a 92 Å distribution. The 10 hr data support the formation of athicker and/or an additional layer with a random Br orientation or multiple Br layer formation. Both the 10 hr reflectivity and XSW data would likely be better fit by multiple Br-PEG-peptide layers, but this is beyond the current scope of the data analysis code.

Figure 5 (a) illustrates the x-ray reflectivity measured for Br-PEG-peptide adsorbed for 2.5 hr on the nonpolar, smooth polar, and rough polar surfaces, with the results of the fits summarized in Table 2 and Table 3. The reflectivity data acquired for the peptide adsorbed on the two polar surfaces are very similar with the variations observed mostly due to differences in film thickness (see below).

Figure 5 (a) shows the oscillations in the reflectivity scan are damped out for the Br-PEG-peptide adsorbed on the nonpolar layer and the fits indicate a layer thickness of <50 Å with a roughness of 30 – 40 Å and a lower relative density. Fitting the subtle oscillations in the nonpolar data is difficult, so the nonpolar fits are less accurate than those for the polar surfaces.

Nevertheless, the nonpolar surface reflectivity results are consistent with a very rough submonolayer or incomplete coverage of the Br-PEG-peptide.

The reflectivity results suggest that the Br-PEG-peptide conformation is distinctly different on the nonpolar versus the polar surface. Figure 5 (b) also displays dramatic differences between the Br fluorescence yield profiles for the Br-PEG-peptide adsorbed for 2.5 hr on the two polar surfaces versus adsorption onto the nonpolar surface. The fluorescence yield profile for Br-PEG-peptide adsorption onto the nonpolar surface displays only one broad peak near the critical angle of Si. The peak reaches a maximum at the critical angle of Si, suggesting that the Br layer is closer to the polystyrene with a broader distribution on the nonpolar surface. The fluorescence yield profile is consistent with an anisotropic orientation of the Br-PEG-peptide on the nonpolar surface, resulting in a broad Br distribution relative to the thickness of the Br-PEG-peptide layer. By contrast, there are two well resolved peaks present in the fluorescence yield profiles of the Br-PEG-peptide adsorbed onto the polar surfaces, suggesting that the Br layer is well above the Si substrate since more than one antinode of the standing wave interacts with the Br layer. As observed for the reflectivity data, the fits to the fluorescence data from the nonpolar surface are the most difficult and therefore the least accurate of those presented. An improved fit to the nonpolar XSW data would likely have been obtained by replacing the Gaussian distribution of Br with a random distribution, but this is beyond the capability of the data analysis code. Nevertheless, the fits indicate a random, low coverage submonolayer of Br-PEG peptide on the nonpolar surface, with a Br-polystyrene distance of 9 Å and a Br distribution width of 17 Å. Oriented adsorption of the Br-PEG-peptide forms only on a polar surface while a patchy, disordered, partial monolayer with an isotropic Br distribution forms on the nonpolar surface.

Slight variations in the thickness and roughness of the underlying films for the smooth versus rough polar surfaces lead to differences in x-ray surface scattering. A shift in the first minimum and period of reflectivity (Figure 5) indicate a difference in the thickness of the two films. A shift of 0.004° in the peaks of the fluorescence yield scans is also observed between the two polar surfaces. Much of this difference can be attributed to changes in the thickness and roughness of the polystyrene layer induced by the different kinetic energy allylamine ions. The effects of ion kinetic energy on polystyrene morphology have been previously discussed for the deposition of gaseous fluorocarbon ions.[16] Briefly, a rougher surface is produced in vacuum (prior to the aqueous adsorption step) by higher kinetic energy ions that simultaneously deposit onto and sputter away the polystyrene layer. This leads to a thinner and rougher polystyrene substrate that nevertheless presents similar polar amine and oxygenated moieties for the subsequent aqueous adsorption of Br-PEG-peptide.

IV. Conclusions

X-ray reflectivity and x-ray standing wave (XSW) fluorescence yield profiles of the Br-PEG-peptide construct provides quantitative information on the position and distribution of the Br marker atom with respect to the adsorption surface. A compact, oriented monolayer of Br-PEG-peptide can be formed with the peptide end adsorbed onto a polar surface and the PEG end terminating with the Br tag extending into the aqueous phase. The distance of the Br atom from the substrate and its narrow spatial distribution is similar to the estimated length of the extended Br-PEG-peptide, indicative of a compact and possibly ordered monolayer. Incomplete multilayers also begins to form on the polar surface after sufficient adsorption time elapses. By contrast, adsorption onto the nonpolar surface is submonolayer, patchy, and highly disordered with an isotropic Br distribution.

The combination of x-ray surface scattering techniques with a novel sample preparation strategy has several advantages for probing molecular adsorption at the liquid-solid interface.

The polystyrene spacer layer shifts the adsorption event beyond the 200 Å critical period of the Si substrate, increasing the information available from XSW. The critical period is characteristic of the material used as the reflecting substrate and is independent of incident x-ray energy. For example, polished gold, silver, and aluminum oxide have critical periods of 77 Å,[38] 97 Å, [19] and 159 Å,[10] respectively. Therefore, a similar spacer layer would be required with any of these substrates to obtain angstrom resolution conformation information on interfacial molecular species. Polyatomic ion deposition in vacuum is a versatile technique for chemical modification of polystyrene and many other potential spacer layers[27] that maintains the high spatial uniformity required for x-ray surface scattering.

XSW is advantageous because it is a real space probe of the conformation of adsorbed or surface bound biomolecules on polymeric substrates. These results demonstrate the ability of XSW to study the adsorption of biomolecules at the solid-aqueous interface by the use of chemical tagging of the adsorbate with a heteroatom that fluoresces during x-ray irradiation. This element specific strategy will work under dilute aqueous conditions which make it suited to many applications including the study of biomaterials-protein interactions, DNA and protein arrays, cell-surface interactions, and receptor-ligand interactions. Furthermore, XSW has been demonstrated with a wide range of heteroatoms beyond Br including iodine, iron, zinc, and selenium. The combined use of x-ray reflectivity, XSW, and atomic force microscopy constitute a powerful strategy for the elucidation of the structure of adsorbed biomolecules on surfaces.

Acknowledgements

References

1. Jones FH. Surf. Sci. Rep 2001;42:75.

2. Castner DG, Ratner BD. Surf. Sci 2002;500:28.

3. Kasemo B. Surf. Sci 2002;500:656.

4. Leonard, EF.; Turitto, VT.; Vroman, L., editors. Blood in Contact with Natural and Artificial Surfaces. New York: Ann. N.Y. Acad. Sci.; 1987. p. 516

5. Tengvall P, Lundstrom I, Liedberg B. Biomater 1998;19:407.

6. Elwing H. Biomater 1998;19:397.

7. Koenig AL, Gambillara V, Grainger DW. J. Biomed. Mater. Res 2003;64A:20.

8. Zhang R, Itri R, Caffrey M. Biophys. J 1998;74:1924. [PubMed: 9545053]

9. Abruna, HD. X-rays as probes of electrochemical interfaces. In: Bockris, JOM.; White, RE.; Conway, BE., editors. Modern Aspects of Electrochemistry. New York and London: Plenum Press; 1989. p. 265

10. Trainor TP, Templeton AS, Brown GEJ, Parks GA. Lang 2002;18:5782.

11. Dev BN. Radia. Phys. Chem 2004;70:525.

12. Russell TP. Mater. Sci. Rep 1990;5:171.

13. Tidswell IM, Ocko BM, Pershan PS, Wasserman SR, Whitesides GM, Axe JD. Phys. Rev. B 1990;41:1111.

14. Schlossman, ML.; Pershan, PS. X-ray and neutron scattering from liquid surfaces. In: Langevin, D., editor. Light Scattering By Liquid Surfaces and Complementary Techniques. New York: Marcel Dekker; 1992. p. 365

15. Schlossman ML, Synal D, Guan Y, Meron M, Shea-McCarthy G, Huang Z, Acero A, Williams SM, Rice SA, Viccaro PJ. Rev. Sci. Instrum 1997;68:4372.

16. Akin FA, Jang I, Schlossman ML, Sinnott SB, Zajac G, Fuoco ER, Wijesundara MBJ, Li M, Tikhonov A, Pingali SV, Wroble AT, Choi Y, Hanley L. J. Phys. Chem. B 2004;108:9656.

17. Bedzyk MJ, Bilderback DH, Bommarito GM, Caffrey M, Schildkraut JS. Science 1988;241:1788. [PubMed: 3175619]

18. Bedzyk MJ, Bommarito GM, Caffrey M, Penner TL. Science 1990;248:52. [PubMed: 2321026]

19. Wang J, Wallace CJA, Clark-Lewis I, Caffrey M. J. Mol. Biol (1) 1994;237

20. Lin B, Morkved TL, Meron M, Huang Z, Viccaro PJ, Jaeger HM, Williams SM, Schlossman ML. J. Appl. Phys 1999;85:3180.

21. Lin W, Lee T, Lyman PF, Lee J, Bedzyk MJ, Marks TJ. J. Amer. Chem. Soc 1997;119:2205.

22. Wang J. Curr. Opin. Coll. Interf. Sci 1998;3:312.

23. Templeton AS, Trainor TP, Traina SJ, Spormann AM, Brown GE Jr. Proc. Nat. Acad. Sci. U.S.A 2001;98:11897.

24. Elbert DL, Hubbell JA. Annu. Rev. Mater. Sci 1996;26:365.

25. Rezania A, Thomas CH, Branger AB, Waters CM, Healy KE. J. Biomed. Mater. Res 1997;37:9. [PubMed: 9335344]

26. Lateef SS, Boateng S, Hartman TJ, Crot CA, Russell B, Hanley L. Biomater 2002;23:3159.

27. Hanley L, Sinnott SB. Surf. Sci 2002;500:500.

28. Hanley L, Choi Y, Fuoco ER, Akin FA, Wijesundara MBJ, Li M, Tikhonov A, Schlossman M. Nucl. Instr. Meth. Phys. Res. B 2003;203C:116.

29. Choukourov A, Kousal J, Slavinska D, Biederman H, Fuoco ER, Tepavcevic S, Saucedo J, Hanley L. Vacuum 2004;75:195.

30. Ratner, BD. Biomaterials science: An interdisciplinary endeavor. In: Ratner, BD.; Hoffman, AS.; Schoen, FJ.; Lemons, JE., editors. Biomaterials Science: An Introduction to Materials in Medicine. New York: Academic Press; 1996.

31. Shin K, Hu X, Zheng X, Rafailovich MH, Sokolov J, Zaitsev V, Schwarz SA. Macromol 2001;34:4993.

32. Wijesundara MBJ, Ji Y, Ni B, Sinnott SB, Hanley L. J. Appl. Phys 2000;88:5004.

33. Yang BX, Rivers M, Schildkamp W, Eng PJ. Rev. Sci. Instrum 1995;66:2278.

34. Eng PJ, Trainor TP, Brown GEJ, Waychunas GA, Newville M, Sutton SR, Rivers ML. Science 2000;288:1029. [PubMed: 10807569]

35. Krol A, Sher CJ, Kao YH. Phys. Rev. B 1988;38:8579.

36. Brennan S, Cowan PL. Rev. Sci. Instrum 1992;63:850.

37. Wang J, Caffrey M, Bedzyk MJ, Penner TL. J. Phys. Chem 1994;98:10957.

38. Bedzyk MJ, Bommarito GM, Schildkraut JS. Phys. Rev. Lett 1989;62:1376. [PubMed: 10039658]
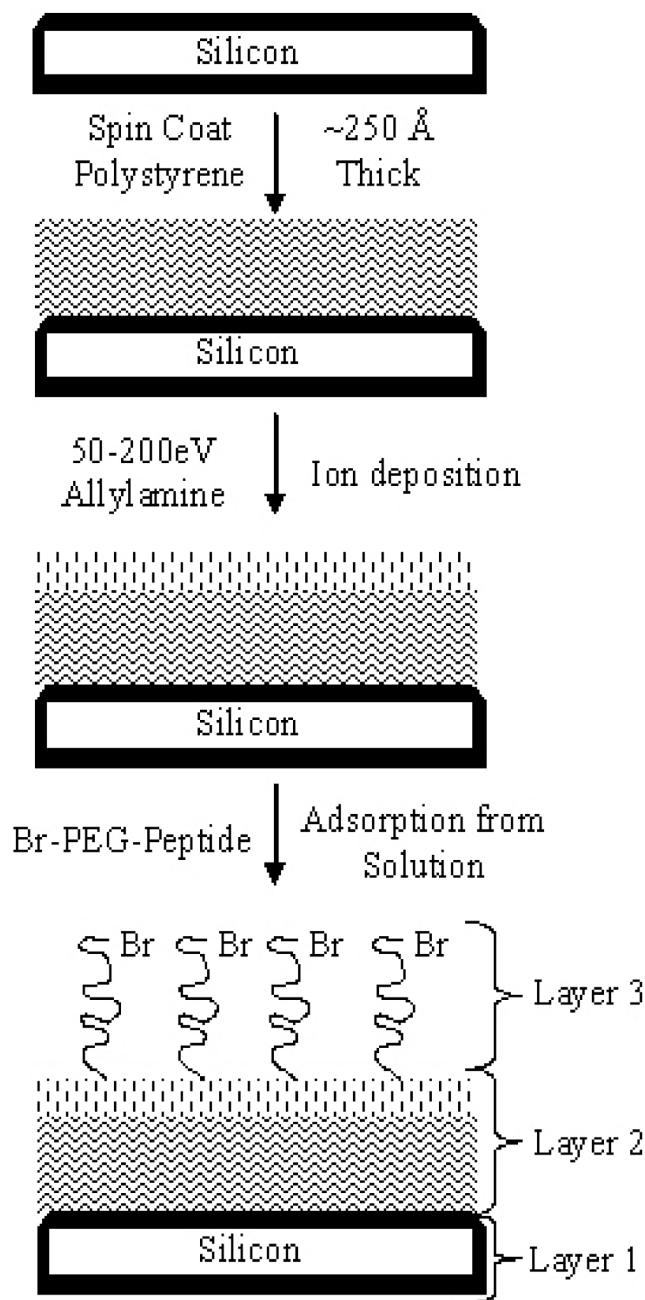
Figure 1.
Schematic for preparation of nonpolar surface consisting of polystyrene layer spin coated onto clean, oxidized Si wafer. Smooth and rough polar surfaces are prepared by deposition of 50 or 200 eV allylamine ions, respectively, to form an oxidized, amine-functionalized polystyrene.
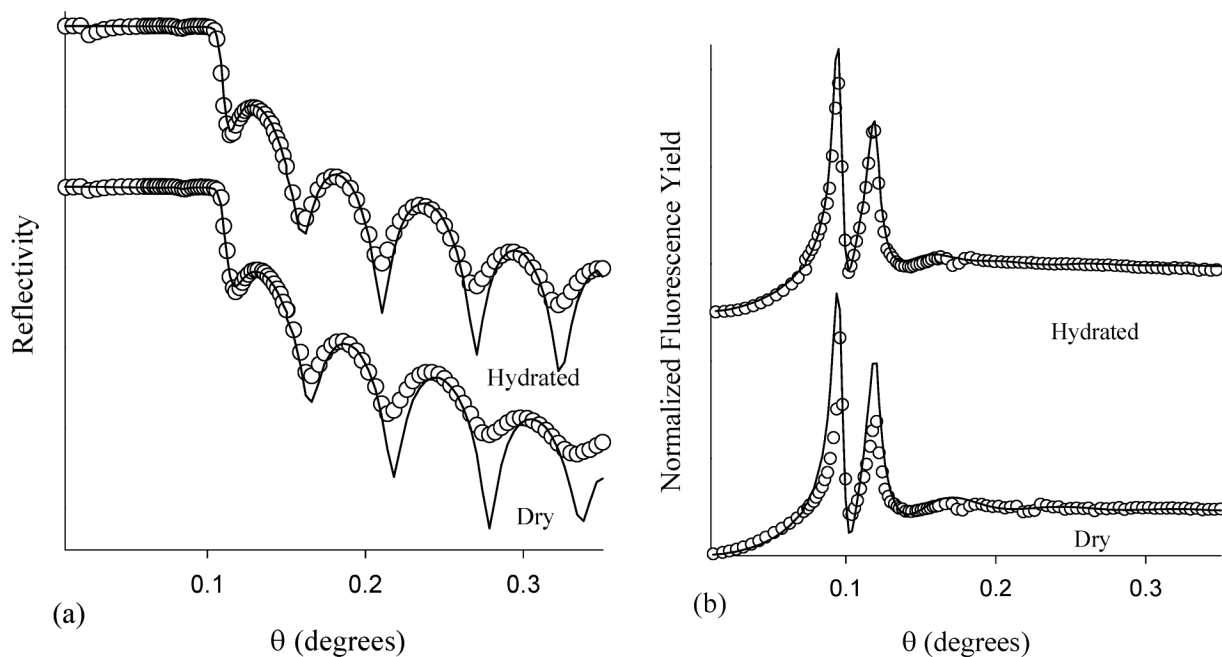
Figure 2.
(a) X-ray reflectivity and (b) Br fluorescence yield of adsorbed Br-PEG-peptide under both dry and hydrated conditions, respectively. Br-PEG-peptide adsorbed for 2.5 hr onto the smooth polar surface (50 eV allylamine ion deposition onto polystyrene).
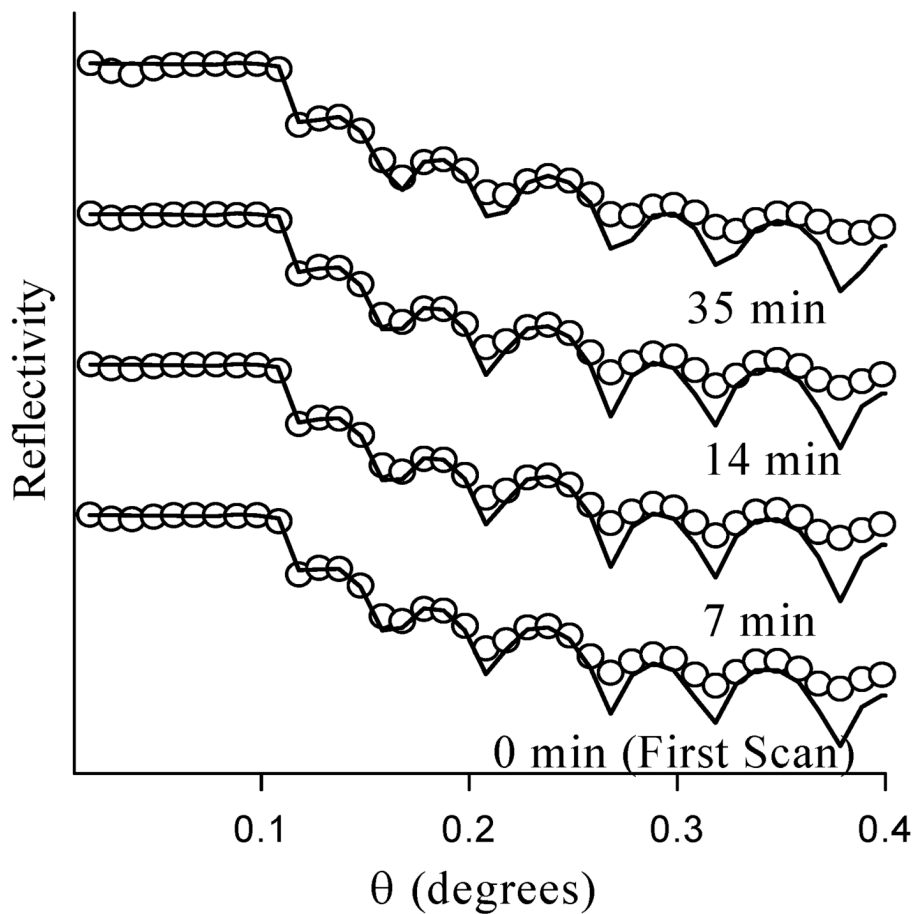
Figure 3.
Evaluation of radiation damage by recording x-ray reflectivity successively from the same spot for Br-PEG-peptide adsorbed onto the smooth polar surface for 2.5 hr. Reflectivity scans separated by the time periods indicated.
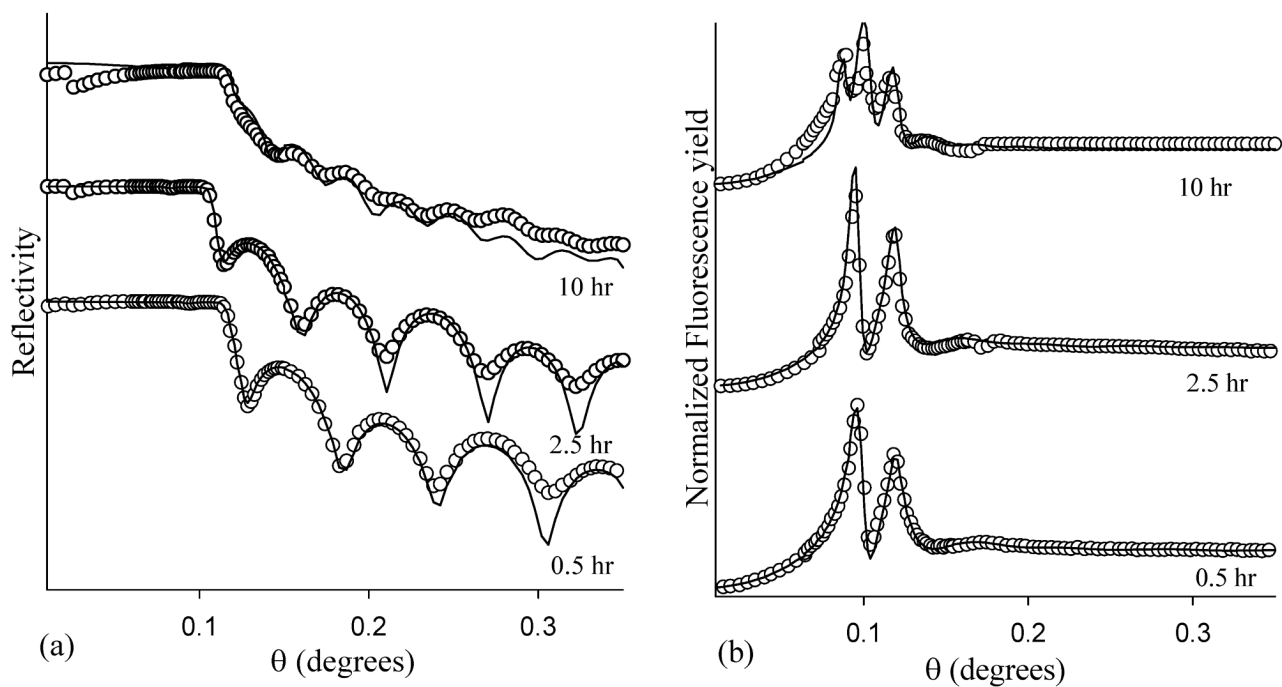
Figure 4.
(a) X-ray reflectivity and (b) Br fluorescence yield as a function of peptide adsorption time.
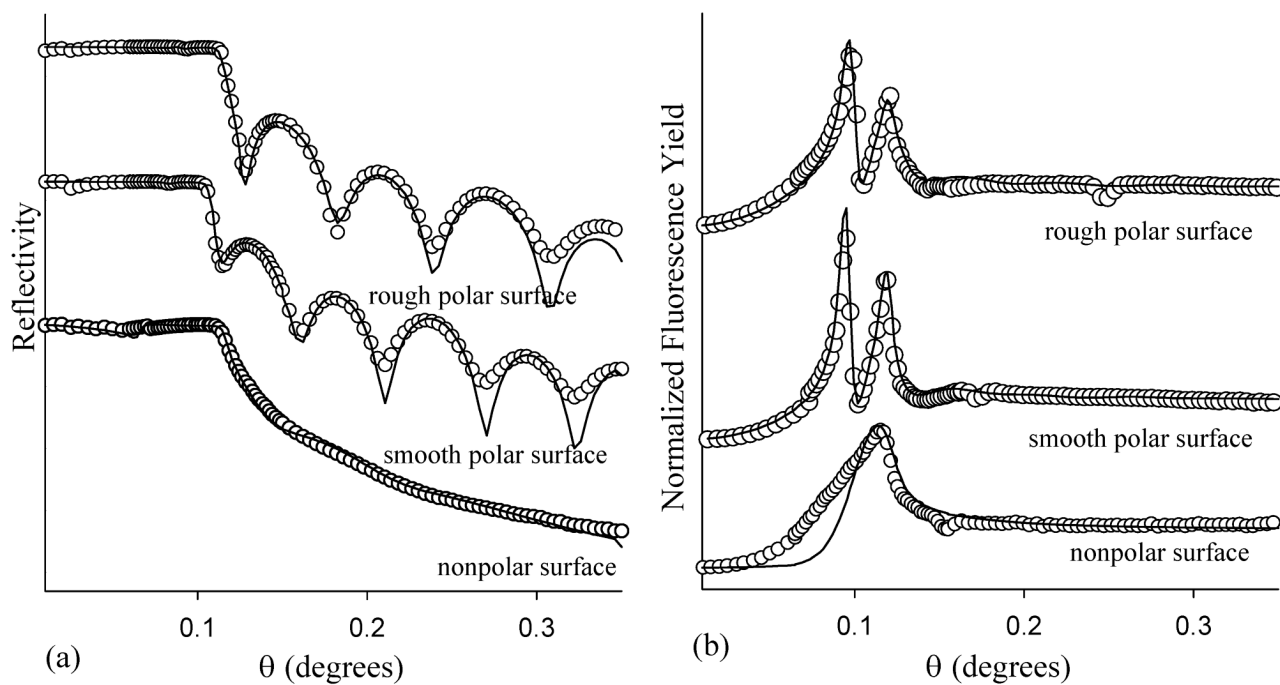Br-PEG-peptide adsorbed for 0.5 – 10 hr onto smooth polar surface.

Figure 5.
(a) X-ray reflectivity and (b) Br fluorescence yield for Br-PEG-peptide adsorbed for 2.5 hr onto the nonpolar, smooth polar, and rough polar surfaces.

Table 1

Elemental content and roughness of the polar and nonpolar surfaces used for adsorption, as well as initial oxidized Si wafer.

	Elemental Content (elemental percentage)[a]				Roughness (RMS, Å)[b]
	Carbon	Oxygen	Silicon	Nitrogen	
Clean Si Wafer	7 ± 1	23 ± 1	70 ± 1	0	2 Å
Nonpolar surface[c]	95 ± 1	5 ± 1	-	-	2 Å
Smooth polar surface[d]	80 ± 1	9 ± 2	-	11 ± 1	3 ± 1 Å
Rough polar surface[e]	79 ± 2	11 ± 1	-	9 ± 1	6 ± 1 Å

[a]Recorded by XPS.

[b]Recorded by AFM.

[c]Native polystyrene.

[d]50 eV allylamine ion deposition on polystyrene.

[e]200 eV allylamine ion deposition on polystyrene.

Table 2

Fitting parameters for Br-PEG-peptide adsorbed on smooth polar surface.

Adsorption Time: Hydration:	0.5 hr Hydrated	2.5 hr Dry	2.5 hr Hydrated	10 hr Hydrated
Layer 1: Si Substrate				
Thickness (Å)	1.00×10^8	1.00×10^8	1.00×10^8	1.00×10^8
Roughness (Å)	2.7	2.7	2.7	2.7
Relative Density	1	1	1	1
Layer 2: Polystyrene + Allylamine				
Thickness (Å)	248 ± 2	250 ± 1	249 ± 1	248 ± 6
Roughness (Å)	3.5 ± 0.8	3.5 ± 0.5	4.0 ± 0.2	3.5 ± 0.4
Relative Density	0.89 ± 0.02	0.91 ± 0.06	0.98 ± 0.05	0.81 ± 0.01
Layer 3: Br-PEG-peptide				
Thickness (Å)	116 ± 5	140 ± 1	156 ± 2	449 ± 8
Roughness (Å)	6 ± 1	4 ± 1	8 ± 1	12 ± 6
Relative Density	0.87 ± 0.02	0.84 ± 0.05	0.89 ± 0.02	0.64 ± 0.10
Br-Polystyrene Distance (Å)	108 ± 5	129 ± 1	141 ± 2	332 ± 17
Br Distribution (Å)	13 ± 2	10 ± 1	10 ± 0.5	92 ± 15

Table 3

Fitting parameters for Br-PEG-peptide adsorbed on rough polar and nonpolar surface.

Sample: Adsorption Time: Hydration:	Rough polar 2.5 hr Hydrated	Rough polar 10 hr Hydrated	Nonpolar 2.5 hr Hydrated
Layer 1: Si Substrate			
Thickness (Å)	1.00×10^8	1.00×10^8	1.00×10^8
Roughness (Å)	2.7	2.7	2.7
Relative Density	1	1	1
Layer 2: Polystyrene + Allylamine Layer (rough polar only)			
Thickness (Å)	222 ± 0.1	221 ± 0.2	250 ± 1
Roughness (Å)	5 ± 1	8 ± 0.1	10 ± 2
Relative Density	0.87 ± 0.01	0.87 ± 0.01	0.75 ± 0.1
Layer 3: Br-PEG-peptide			
Thickness (Å)	137 ± 3	313 ± 14	<50
Roughness (Å)	8 ± 1	16 ± 4	$30 - 40$
Relative Density	0.91 ± 0.02	0.73 ± 0.04	0.48 ± 0.04
Br-Polystyrene Distance (Å)	130 ± 6	204 ± 16	9 ± 5
Br Distribution (Å)	11 ± 2	104 ± 10	17 ± 5